Kirkuk University Journal /Scientific Studies (KUJSS)
Volume 10, Issue 3, September 2015 , p.p(242-258)
ISSN 1992 – 0849

Petrogenesis of metabasalt rocks in the Bulfat complex, Kurdistan region, Iraqi Zagros Suture Zone

Sarmad A. Ali [1&2]

[1]Department of Applied Geology, College of Science, University of Kirkuk, 36001, Iraq

[2]School of Earth and Environmental Sciences, University of Wollongong, Wollongong, New South Wales, Australia

sarmad@uow.edu.au

Received date: 6 / 4 / 2015 **Accepted date: 13 / 5 / 2015**

ABSTRACT

Metabasaltes are exposed in the Bulfat complex north of Qaladeza that is a part of the Northwestern Zagros Suture Zone (NZSZ).Petrographic and geochemical study of metabasaltes have been conducted in order to provide insights into the origin and evolution of magmatism found at Neotethyian subducted plate margins and to determine their protolith nature and geodynamic setting. The whole rock chemistry indicates basalt to andesite composition for the metabasaltes. The geochemical investigation strongly suggests that the metabasaltes are derived from calic alkaline basalt and were emplaced in arc tectonic setting.

Keywords: *Petrogenesis, Collision zone, Bulfat Complex, Iraq.*

Kirkuk University Journal /Scientific Studies (KUJSS)
Volume 10, Issue 3, September 2015 , p.p(242-258)
ISSN 1992 – 0849

نشوئية الصخور البازلتية المتحولة في معقد بولفات، أقليم كردستان ، نطاق درز زاكروس العراقي

سرمد عاصي علي

جامعة كركوك / كلية العلوم / قسم الجيولوجيا التطبيقية

sarmad@uow.edu.au

تاريخ استلام البحث: 6 / 4 / 2015 تاريخ قبول البحث: 13 / 5 / 2015

الملخص

تنكشف صخور البازلت المتحولة في معقد بولفات شمال قلعة دزة الواقع ضمن الجزء الشمال الغربي لنطاق درز الزاركروسي، تمت دراسة بتروغرافية وجيوكيميائية لصخور البازلت المتحول لغرض معرفة اصل وتطور الصهير المتكون نتيجة لغوران جزء من القشرة المحيطية لبحر التيثس الجديد وتحديد نوعية صخور الام وجيوديناميكية المنطقة ، اثبتت التحريات الجيوكيميائية بان الصخور هي سلسة تبدا بالبازلت وتنتهي بالاندسايت وتشير الدلائل الجيوكيميائية ايضاً بانها سلسة شبة قلوية تموضعت في بيئة القوس البركاني.

الكلمات الدالة: نشوئية، نطاق التصادم، معقد بولفات، العراق.

1.INTRODUCTION

Jabal Bulfat, 30 km east of Qala Deza City, Kurdistan region, NE Iraq, is a deeply dissected mountainous area composed generally of a wide spectrum of igneous rocks referred to as the Bulfat Complex [1]. It forms a major part of the Upper Allochthon 'ophiolite-bearing terraine' and encompasses a volcanosedimentary unit – the 'Gemo-Qandil Sequence'. This sequence was originally referred to the Bulfat Group by [2]. The Gemo-Qandil Sequence has experienced a medium-grade regional metamorphism overprinted by a high-grade contact metamorphism during Paleogene [1]. The complex is composed largely of basic rocks intruded into the Bulfat group, the contact area is represented by sheet intrusion along bedding planes of the metasediments.

Kirkuk University Journal /Scientific Studies (KUJSS)
Volume 10, Issue 3, September 2015 , p.p(242-258)
ISSN 1992 – 0849

Minor body of ultrabasic rocks and very limited occurrence of acid differentiates are also present. Xenoliths of the country rocks and very high grade thermal metamorphism up to the pyroxene hornfels facies is characteristic for the Bulfat complex [3]. In this paper, the petrogenesis of Qaladeza metabasaltes has been demonstrated. This was achieved via integrated whole-rock petrography and geochemistry.

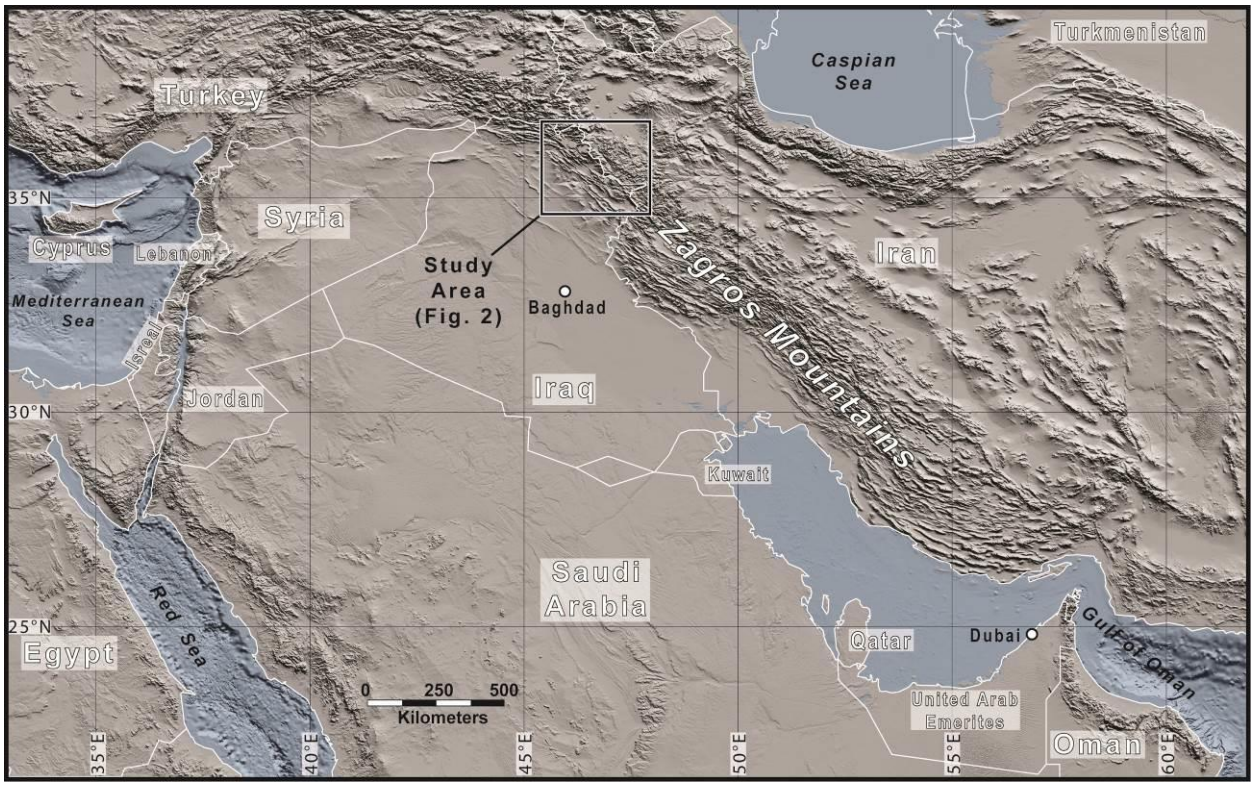

Figure (1): Location of study areas within the Zagros Suture Zone (Ali et al. 2012).

2.GEOLOGICAL BACKGROUND

The study area lie between longitude 45^{o} $14^{/}$ $39.54^{//}$ E and latitudes 36^{o} $11^{/}$ $55.3^{//}$ N, and it is situated along the Iraq-Iran- border,30 km east Qala Deza City, Kurdistan region, NE Iraq. The study area contains unexploded landmines, limiting sampling to the boundary of main roads. The study area forms part of the Western Zagros Fold-Thrust Belt, which developed as a response to collision of the Arabian and Iranian plates [1] Figures (1 and 2), and it is an integral part of the Zagros suture zone [4]. The complex comprises allochthonous detachment of the Albian-

Kirkuk University Journal /Scientific Studies (KUJSS)
Volume 10, Issue 3, September 2015 , p.p(242-258)
ISSN 1992 – 0849

Cenomanian Gemo-Qandil Sequence (Upper Allochthon) and the Paleocene-Eocene Walash Volcano-sedimentary Sequence (Lower Allochthon; [5&6]). On the basis of recent studies [4, 5&6], these two allochthonous sheets were juxtaposed and amalgamated into a single nappe (Walash-Penjween Subzone) following the closure of the Neo-Tethys. Coeval volcanic activity of Walash-Naopurdan 'Lower Allochthon' with the multiphase intrusion of the Bulfat Complex is common along the entire length of the Iraqi Zagros Suture Zone and the volcanic activity represents widespread arc-back arc volcanism during the Paleogene. With the exception of the Bulfat Complex, the remainder of the Lower Allochthon does not show any similar intrusive features [7]. Field evidence shows that the nappe which incorporates the two amalgamated sheets rests on top of various units: Tertiary Mollasses (Tertiary Red Beds), Neoautochthonous flysch (Maastrichtian) and parautochthonous radiolarite (Albian-Cenomanian; [8]). Exhumation of the Bulfat Complex occurred through the formation of nappes in a continental collision [7] that terminated during the Middle Miocene [8].

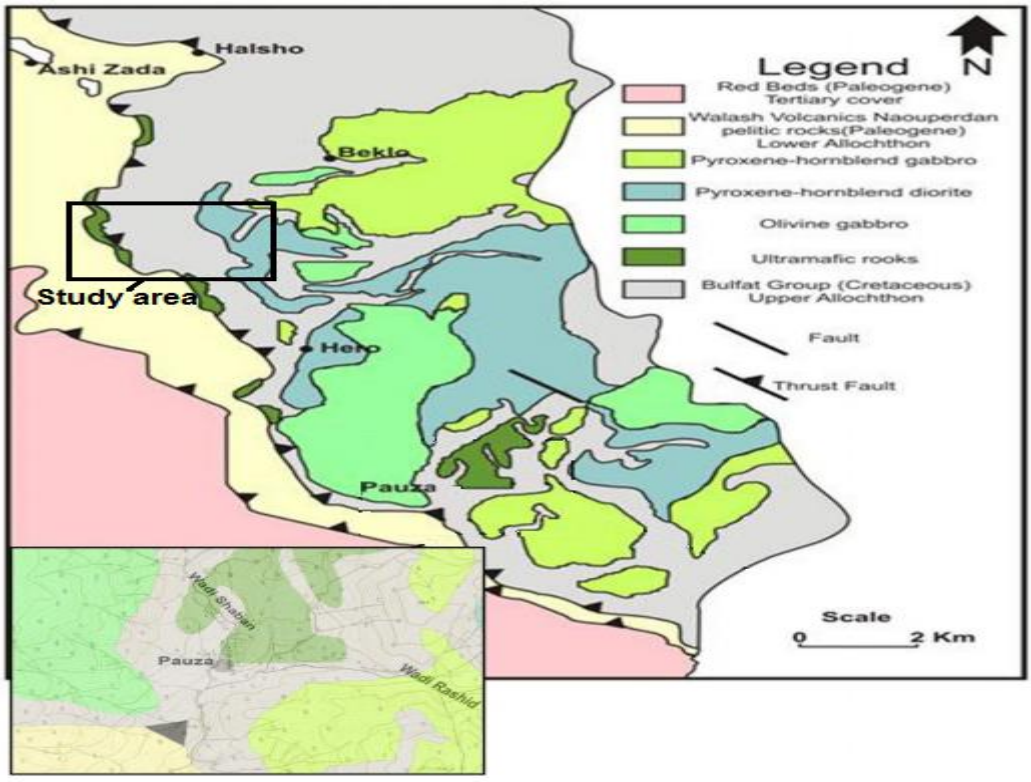

Figure (2): Geological Map of Bulfat Complex, Qala Deza, NE Iraq (Modified from Aswad et al, 2013).

Kirkuk University Journal /Scientific Studies (KUJSS)
Volume 10, Issue 3, September 2015 , p.p(242-258)
ISSN 1992 – 0849

3.ANALYTICAL METHODS

X-ray fluorescence (XRF) analysis was carried out with a Spectro-Analytical Instrument (XEPOS) energy-dispersive spectrometer fitted with a Si-diode detector at School of Earth and Environmental Sciences, University of Wollongong, following the methods of [9]. Major elements were measured on samples fused with Li borate while trace elements were analyzed from pellets bonded with Polyvinyl acetate. Calibration was made against a wide range of international reference materials and laboratory standards previously calibrated against synthetic standards. Loss-on-ignition was determined by heating a separate aliquot of rock powder at 1000°C. The samples were analyzed for rare earth elements (REE) and other trace elements at the Australian Laboratory Services (ALS), Brisbane, Australia, by inductively coupled plasma–mass spectrometry (ICP-MS) on dissolved aliquots of powder. Microprobe analyses were carried out on polished thin-sections using a fully automated Cameca SX100 electron microprobe at Macquarie University, fitted with five wavelength dispersive spectrometers (WDS) and a Princeton Gamma Tech (PGT) energy dispersive system (EDS). Further analytical details are provided by [10].

4.PETROGRAPHY AND MINERAL CHEMISTRY

The metabasalt rocks have mostly grey to brownish grey weathering. Study of 10 thin-sections shows that these rocks display decussate, porphyritic, and intergranular textures Figures (3A, 3B &3C).Phenocrysts include altered plagioclase, Amphibole, Biotite, clinopyroxene, and iron oxide**.** Secondary minerals such as chlorite, serpentine, sericite and epidote are present in most samples.

4.1. Plagioclase

Microprobe analyses of plagioclase in the most metabasalt rocks samples are provided in Table (1). The anorthitic component (An) of normally zoned plagioclase crystals ranges between (An 5to An 98) for the most samples, whereas orthoclase is observed only in one sample (QL3). There are noticeable differences between the compositions of plagioclase crystals in the various rock groups ranging from Anorthite to Albite Table (1) and Figure (3D). In some samples, plagioclase crystals are wholly replaced by finer-grained epidote and/ or sericite.

Kirkuk University Journal /Scientific Studies (KUJSS)
Volume 10, Issue 3, September 2015 , p.p(242-258)
ISSN 1992 – 0849

4.2. Amphibole

Primary amphibole is the most abundant mafic mineral in the studied rocks. It is essentially homogeneous in composition, and corresponds mostly to calcic amphibole (e.g. Magnesio-hornblende) Table (1) & Figure (3E) with exception of sample (QH4) which it also has sodic-calcic (winchite) Figure (3F).

4.3. Pyroxene

Only one clinopyroxene grain was observed in the QH9 sample with diopside composition Table (1) & (3F).

4.4. Iron oxides

Iron oxides are found as fine crystals randomly scattered in the groundmass. Three spots in three samples (QL3, QH8 &QH4) were analyzed and the formulae were calculated on the basis of 6 oxygen Table (1) & Figure (3G), all with aliment composition.

4.5. Biotite

Textural and petrological studies indicate that the biotite in QL3. The composition of the biotite is Fe- and Ti-rich and Al-poor, taken in conjunction with (Fe exclusively present as Fe^{2+}). Accordingly, the biotite is classified as Fe-biotite on the Foster classification diagram [11], Table (1) & Figure (3H).

Kirkuk University Journal /Scientific Studies (KUJSS)
Volume 10, Issue 3, September 2015 , p.p(242-258)
ISSN 1992 – 0849

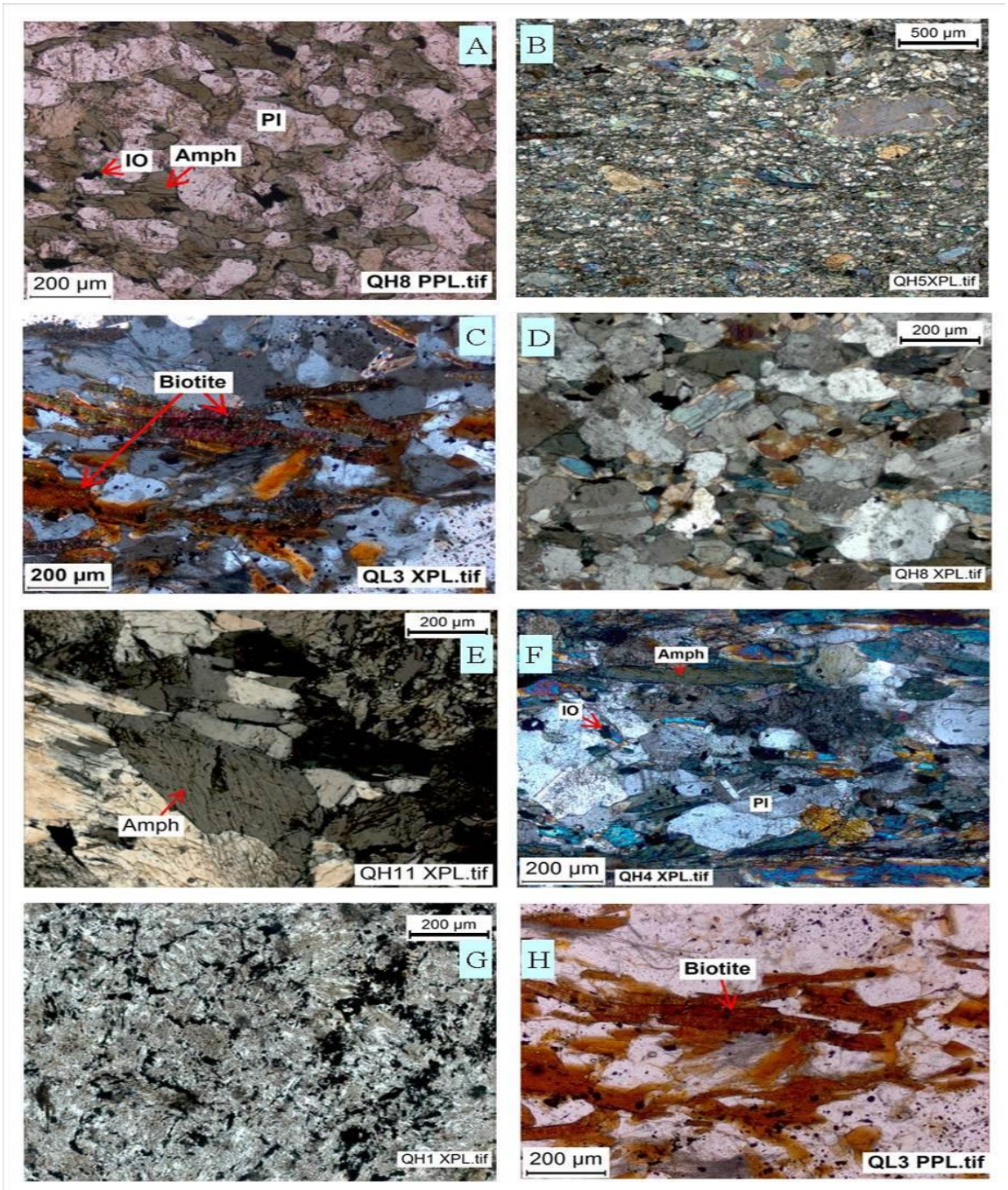

Figure(3): Photomicrographs of selected samples used for mineral microprobe analysis (polarized light). (A-H). A, B&C: decussate, porphyritic and intergranular textures. D: Plagioclase grains with different compassion in sample (QH8). E: Magnesio-hornblende in sample QH11. F: clinopyroxene and winchite (sodic- calcic amphibole) grains in sample QH4. G: Iron oxides in the matrix of sample QH1. H: Biotite grains in sample QL3.

Kirkuk University Journal /Scientific Studies (KUJSS)
Volume 10, Issue 3, September 2015 , p.p(242-258)
ISSN 1992 – 0849

5.GEOCHEMISTRY

5.1 Major Elements

The bulk chemistry of Qaladeza metabasalts is deduced from the 10 analyses Table (2). The Qaladeza metabasalts volcanic and subvolcanic rocks are all mafic to intermediate. It shows loss-on-ignition values ranging from 1.13 to 2.9 with exception of one sample QH1 (10.8) Table (2). Silica content ranges between 40.49 to 61.84%. SiO_2 shows a significant negative correlation with MgO Table (2) & Figure (4a). Variations (wt%) for other oxides are Al_2O_3 1.14–22.28; CaO 0.63–15.2; MgO 2.79–37.86; Fe_2O_3 t (as total iron) 4.2–9.5; TiO 0.075–1.78; P_2O_5 0.04–0.43; and MnO 0.06–0.16 Table (2).

Most major oxides display a clear negative or positive correlation with increasing MgO content, reflecting the vital role of fractional crystallization processes during the evolution of the Qaladeza metabasalt rocks. The trends for CaO, SiO_2, and TiO_2 versus MgO are suggestive of fractionation of clinopyroxene, plagioclase, amphibole, and Ti-Fe oxides Figure (4A, B & C). In the AFM (A [Na_2O + K_2O], F [FeOt], M [MgO]) triangle, all the Qaladeza metabasalts samples fall in the calc-alkaline field of [12], Figure (5A), and hence most samples can be classifi ed ascalc-alkaline andesites and andesites. The Qaladeza metabasalts volcanic and subvolcanic samples plot in the calc-alkaline and Ocean island basalt fields on the TiO_2-MnO-P_2O_5 diagram of [13]. Most samples have low K contents (except two samples that fall in a medium-K range-QL3 and QH12) Figure (5B). The Qaladeza metabasalt are all classified as basalts, using the total alkalies-silica (TAS) diagram of [19] Figure (5D).

5.2 Trace Elements

The ranges for Cr, Ni, and Co in the Qaladeza metabasalt samples are 140– 2478, 44.8–2041, and 5.3–115.4 ppm, respectively Table (2). Cr is highly compatible and is concentrated in clinopyroxene, and spinel [14], and hence it shows a significant positive correlation with MgO Figure (4D) . Ni shows positive correlation with MgO Figure (4E) in all samples. The Qaladeza metabasalt samples contain vanadium in the range from 22.9–466.3 ppm. Vanadium shows a strong fractionation into Fe–Ti oxides [14]. In addition, vanadium is incorporated into pyroxene, amphibole, and biotite [15]. It shows a significant positive correlation with Fe_2O_3 in Qaladeza metabasalt which is related to the similarity in chemical behavior between V and Fe and the

Kirkuk University Journal /Scientific Studies (KUJSS)
Volume 10, Issue 3, September 2015 , p.p(242-258)
ISSN 1992 – 0849

presence of relict magmatic Fe–Ti oxides in the rocks (Figure not shown). The incompatible high field strength elements (HFSEs) such as Zr, Y, Nb, show clearer negative correlation trends with MgO Figure (4F) .The Nb-Zr-Y, diagram [15] is useful for distinguishing different tectonic settings of gabbros. In these diagrams, Qaladeza metabasalt show an affinity with volcanic basalt arc (VAB) Figure (5C).

Table (1): Selective electron microprobe analyses of Feldspar (F), Amphibole (Amp), Pyroxene (Px), Biotite (Bio)and Iron oxides (IO).

sample	QL3 F	QH8	QH4	sample	QH5 Amp	QH11	QH4	sample	QH9Px	sample	QL3 Bio	sample	QL3 IO
SiO2	63.59	59.85	57.07	SiO2	48.78	43.22	56.28	SiO2	52.63	SiO2	33.45	TiO2	53.22
Al2O3	18.31	24.01	26.05	TiO2	0.17	1.06	0.03	TiO2	0.05	TiO2	3.09	Cr2O3	0.07
FeO	0.05	0.11	0.19	Al2O3	8.03	11.95	15.52	Al2O3	0.62	Al2O3	19.32	Al2O3	0.00
CaO	0.03	6.22	8.83	Cr2O3	0.02	0.07	0.00	Cr2O3	0.01	FeO	21.75	FeO	41.24
Na2O	1.49	7.99	6.70	FeO	8.46	9.43	6.60	FeO	6.86	MnO	0.22	MnO	1.46
K2O	14.84	0.07	0.04	MnO	0.17	0.15	0.09	MnO	0.25	MgO	5.76	MgO	0.09
No Oxyg	32.00			MgO	16.20	15.05	7.89	MgO	14.22	CaO	0.00	CaO	0.02
Si	11.93	10.84	10.36	CaO	12.27	11.75	7.89	CaO	24.77	Na2O	0.12	SiO2	0.05
Al	4.05	5.12	5.57	Na2O	0.78	2.43	5.13	Na2O	0.16	K2O	8.95	Ti	2.07
Fe(ii)	0.01	0.02	0.03	K2O	0.03	0.20	0.10	K2O	0.02	Si	5.31	Cr	0.00
Ca	0.01	1.21	1.72	Si	7.07	6.34	7.57	Total	99.59	Al (iv)	2.69	Al	0.00
Na	0.54	2.81	2.36	Al (iv)	0.93	1.66	0.43	Si	1.96			Nb	0.00
K	3.55	0.02	0.01	Al (vi)	0.44	0.41	2.04	Ti	0.00	Al (vi)	0.93	Fe	1.78
An	0.13	29.96	42.02	Fe(iii)	0.42	0.59	0.00	Al	0.03	Ti	0.37	Mn	0.06
Ab	13.20	69.64	57.76	Ti	0.02	0.12	0.00	Fe^{+3}	0.06	Fe(ii)	2.89	Mg	0.01
Or	86.67	0.40	0.21	Fe(ii)	0.60	0.57	0.74	Cr^{+3}	0.00	Mn	0.03	Ca	0.00
				Mn	0.02	0.02	0.01	Fe^{+2}	0.15	Mg	1.36	Si	0.00
				Mg	3.50	3.29	1.58	Mn	0.01	Ca	0.00	TOTAL	3.93
				Ca	1.90	1.85	1.14	Mg	0.79	Na	0.04	No Oxyg	6.00
				Na	0.22	0.69	1.34	Ca	0.99	K	1.81		
				K	0.01	0.04	0.02	Na	0.01	Cl	0.00		
				TOTAL	15.13	15.57	14.87	K	0.00	F	0.00		
				Type	Magnesio	Magnesio	Winchite	Wo	51.24	TOTAL	15.43		
					hornblende	hastingsite		En	40.94				
								Fs	7.83				

Kirkuk University Journal /Scientific Studies (KUJSS)
Volume 10, Issue 3, September 2015 , p.p(242-258)
ISSN 1992 – 0849

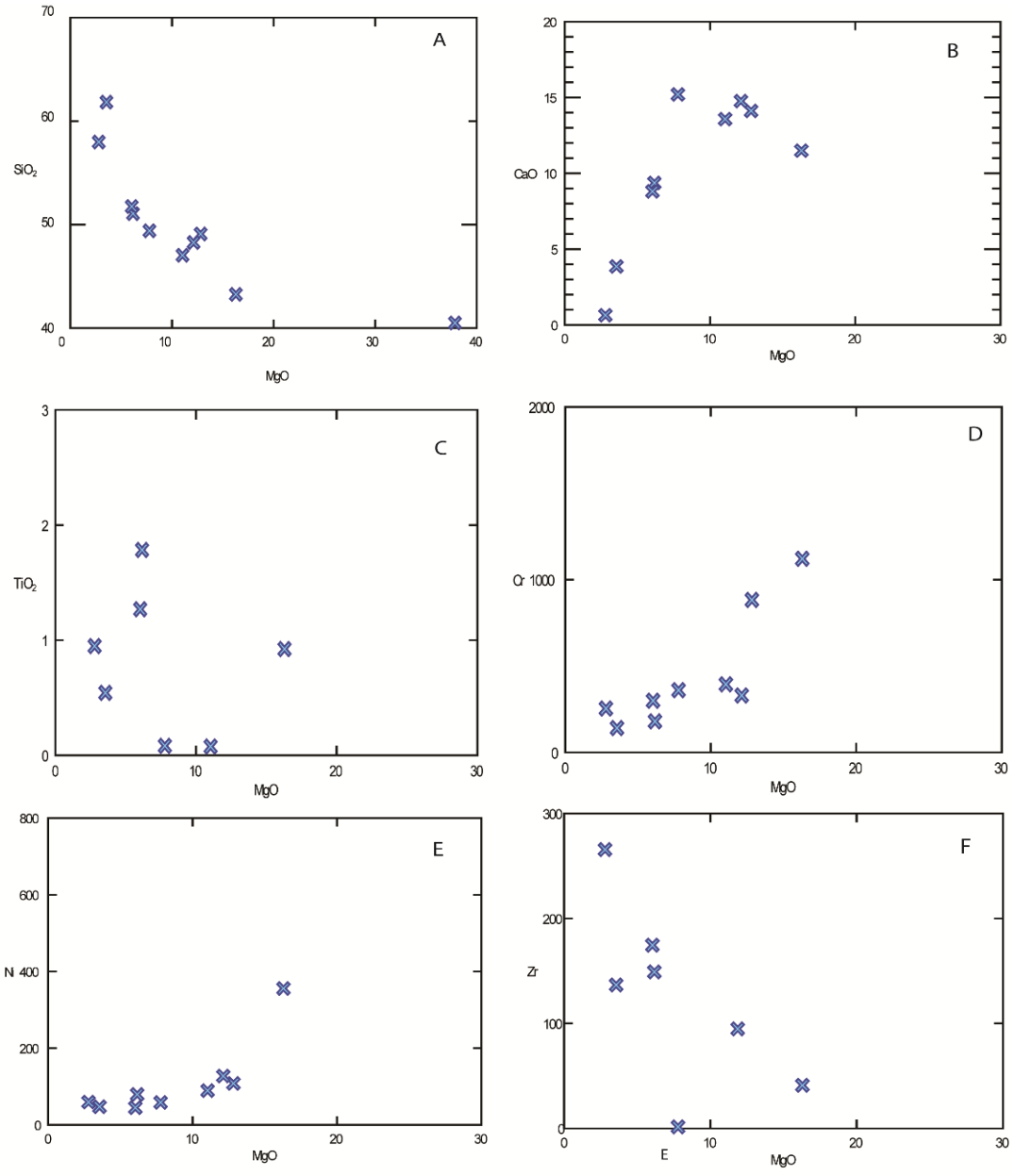

Figure (4): Selected binary diagrams showing major and trace elements variation of Qaladeza metabasalt rocks.

Kirkuk University Journal /Scientific Studies (KUJSS)
Volume 10, Issue 3, September 2015 , p.p(242-258)
ISSN 1992 – 0849

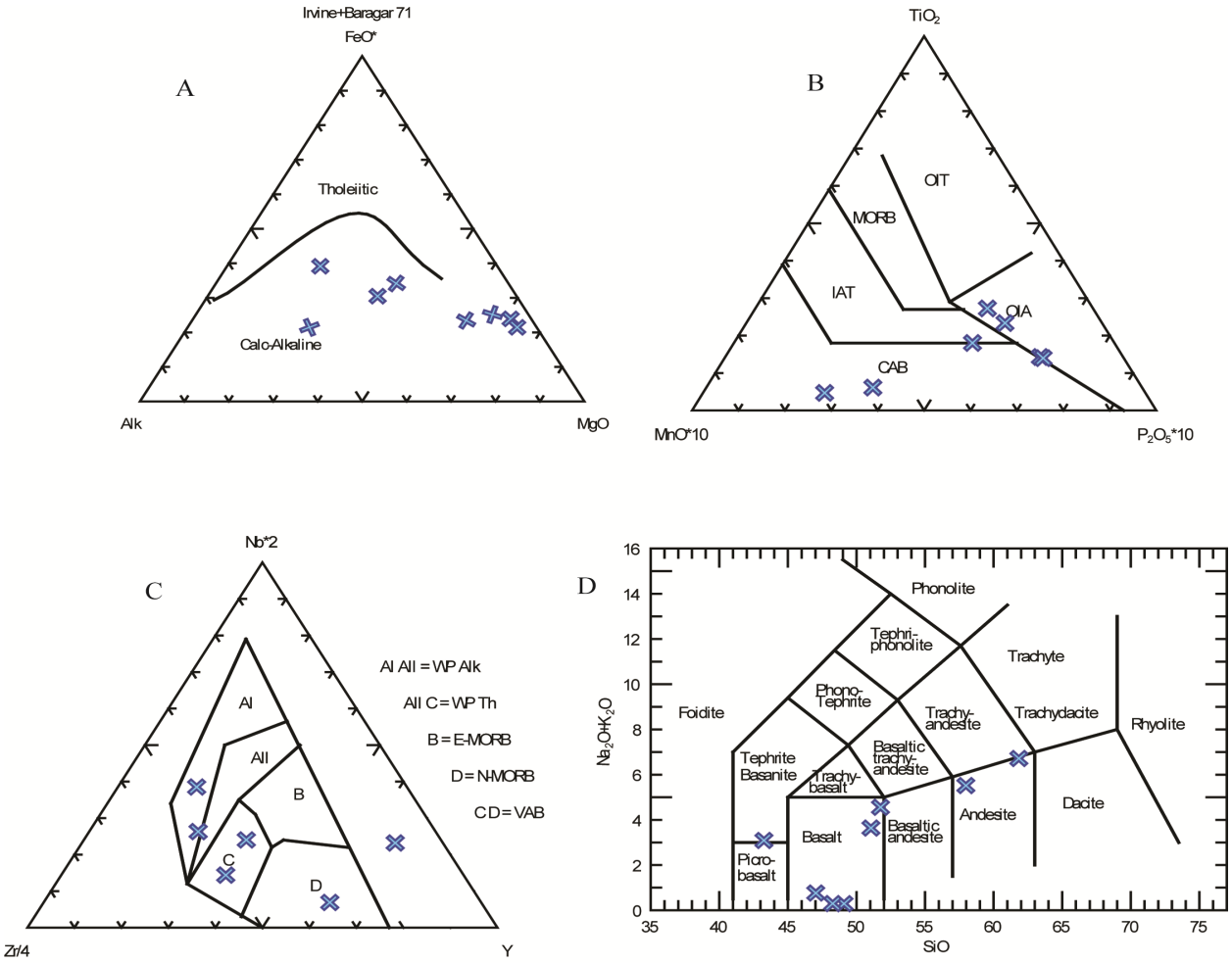

Figure (5): Tectonic discrimination digrams A B and C, afters [12, 13 and 15]. D is the Diagram to discriminate different rock type in the Qaladeza metabasalt rocks after [19].

Kirkuk University Journal /Scientific Studies (KUJSS)
Volume 10, Issue 3, September 2015 , p.p(242-258)
ISSN 1992 – 0849

Table (2): Major and trace element analaysis from Qaladeza metabasalt rocks, n.d. not detected.

Sample	QH1	QH2	QH4	QH5	QH7	QH8	QH9	QH11	QH12	QL3
SiO2	40.49	49.09	51.06	47.03	48.27	51.75	49.4	43.25	61.84	57.98
TiO2	0.00	0.00	1.78	0.08	0.00	1.27	0.08	0.92	0.54	0.95
Al2O3	1.145	16.03	18.07	18.24	17.41	18.59	21.52	14.22	17.05	22.28
Fe2O3t	9.30	6.10	7.58	6.29	6.24	7.03	4.68	9.57	4.25	7.65
MnO	0.10	0.11	0.15	0.11	0.10	0.11	0.08	0.12	0.07	0.16
MgO	37.86	12.83	6.17	11.04	12.13	6.04	7.79	16.29	3.56	2.80
CaO	0.10	14.11	9.36	13.57	14.76	8.80	15.20	11.49	3.86	0.64
Na2O	0.02	0.15	3.50	0.41	0.19	4.30	0.02	2.88	5.02	0.78
K2O	0.01	0.14	0.14	0.35	0.10	0.26	0.10	0.20	1.69	4.74
P2O5	0.39	0.09	0.33	0.04	0.05	0.30	0.05	0.44	0.27	0.27
LOI	10.8	1.46	2.21	2.9	1.68	1.81	1.31	1.77	2.15	2.09
total	100.19	100.11	100.35	100.06	100.93	100.27	100.20	101.15	100.30	100.33
Mg#	0.89	0.81	0.62	0.78	0.79	0.63	0.77	0.77	0.62	0.42
V	30.8	186.2	172.9	133.9	184	160.7	127.6	446.3	22.9	59.1
Cr	2478	882.6	179.9	394	329.5	298.9	360.4	1121	140.8	253.9
Co	115.4	n.d.	66.1	37.8	n.d.	10.4	8.1	n.d.	5.3	44.1
Ni	2041	107.9	79.1	89.3	127.3	44.8	58.4	355.5	47.3	59.4
Cu	27.9	9.4	222.3	6	6.1	30.2	1.1	n.d.	23.4	9
Zn	54.8	31.2	52.6	100.7	26.1	56.5	28.5	41.9	46.3	123.4
Rb	n.d.	2.1	1.2	8.7	0.9	1.6	0.3	0.6	23.6	186
Sr	1.3	102.7	332.5	219	99.8	238.5	77	119.9	429	132.7
Y	n.d.	1.3	31.1	1.8	2	30.2	2.3	19.4	12.8	30.5
Zr	n.d.	n.d.	149	n.d.	n.d.	174.5	1.4	41	136.6	265.6
Nb	0.3	n.d.	10.8	n.d.	n.d.	6.2	0.4	1.1	14.7	17.3
Ba	25.3	20.1	32.7	54.3	22.2	43.5	n.d.	n.d.	271.7	407.5
Hf	7	1.6	2.8	n.d.	1.3	12.3	5.9	8.1	6.5	3

Kirkuk University Journal /Scientific Studies (KUJSS)
Volume 10, Issue 3, September 2015 , p.p(242-258)
ISSN 1992 – 0849

Ta	16.3	n.d.	n.d.	n.d.	n.d.	10.2	13	16.3	1.7	n.d.
Pb	n.d.	0.4	2	5.9	0.4	8	n.d.	n.d.	3.8	39.9
Th	n.d.	n.d.	n.d.	n.d.	n.d.	0.7	n.d.	n.d.	3.3	13.4
U	n.d.	1.1	1.1	3	0.5	1.4	1.2	n.d.	2.1	4.9
Ce	2.2	n.d.	27.2	n.d.	1.5	23.4	n.d.	11.3	31.5	99
Cs	0.02	0.26	0.14	0.99	0.07	0.03	n.d.	0.01	0.07	12.8
Dy	0.12	0.23	5.34	0.28	0.34	5.03	0.4	3.42	1.92	5.63
Er	0.09	0.2	3.6	0.22	0.29	3.38	0.32	2.18	1.23	3.96
Eu	0.03	0.05	1.78	0.07	0.08	1.45	0.1	1.24	0.92	1.88
Gd	0.18	0.18	5.7	0.19	0.25	5.07	0.32	3.92	2.62	6.53
Ho	0.04	0.07	1.25	0.08	0.09	1.16	0.11	0.78	0.43	1.3
La	1.4	0.5	11.6	n.d.	0.8	9.5	n.d.	3.1	17.4	51.5
Lu	0.02	0.03	0.44	0.04	0.05	0.43	0.05	0.24	0.17	0.55
Nd	0.9	0.2	17.3	0.3	0.7	14.5	0.3	10.5	13.2	40.7
Pr	0.28	n.d.	3.9	n.d.	0.14	3.29	0.03	2.03	3.65	11.5
Sm	0.09	0.06	4.36	0.1	0.14	3.83	0.13	3.11	2.51	7.43
Tb	0.02	0.04	0.94	0.04	0.05	0.87	0.06	0.62	0.38	0.99
Tl	n.d.	n.d.	n.d.	n.d.	n.d.	n.d.	n.d.	n.d.	n.d.	0.6
Tm	0.02	0.04	0.52	0.03	0.05	0.5	0.06	0.3	0.19	0.58
Yb	0.09	0.17	3.12	0.24	0.31	2.93	0.29	1.76	1.16	3.74

5.3 Rare earth elements and spider diagrams

The chondrite-normalized REE patterns for all the Qaladeza metabasalt are separated into two groups, the first one (QH4,QH8,QH11,QH12 and QL3) with enrichment in light REEs (LREEs) while second one (QH1,QH2 QH5 and QH7) with less enrichment in light REEs (normalizing values from [16]. Overall flat-lying with very slight enrichment of the light REE (LREE) Figure (6A). Such flat-lying patterns resemble those formed in island-arc and subduction-related settings with [17&18]. The metabasalt rocks show prominent negative Nb anomalies with respect to the neighboring fluid-mobile incompatible elements on normal-type mid-oceanic ridge basalt

Kirkuk University Journal /Scientific Studies (KUJSS)
Volume 10, Issue 3, September 2015 , p.p(242-258)
ISSN 1992 – 0849

(NMORB)-normalized plot Figure (6B). In addition, on the most incompatible elements (i. e. Cs, Rb, Ba, Th and U) are seen to be highly variable in abundance, presumably due to seawater alteration and/or regional metamorphism.

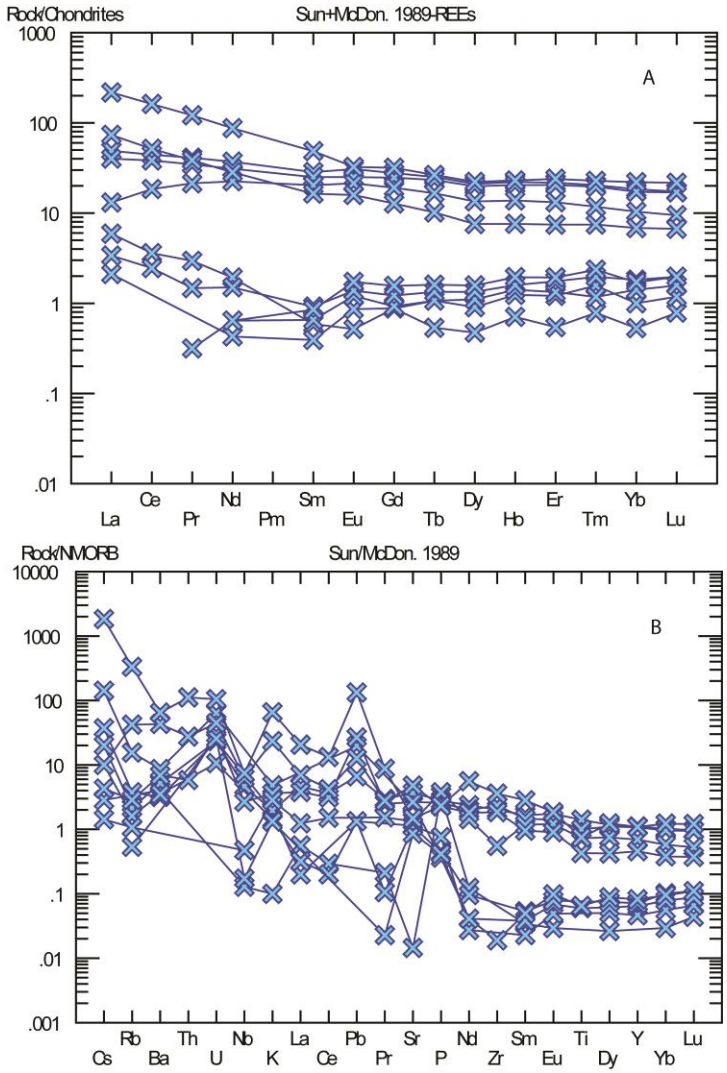

Figure (6): Chondrite nd NMORB plots, chondrite values are from [16], and NMORB values are from [20].

Kirkuk University Journal /Scientific Studies (KUJSS)
Volume 10, Issue 3, September 2015 , p.p(242-258)
ISSN 1992 – 0849

6.DISCUSSION AND CONCLUSIONS

The petrographic study shows that these rocks were affected by metamorphic alteration under greenschist facies conditions and that is clear in most samples, particularly, in QH1 which it has high loss- on-ignition value due to high content of serpentine minerals (e.g. lizardite). Despite superimposed secondary alteration, clear igneous geochemical trends are preserved the Qaladeza metabasalt are all mafic to intermediate, with MgO showing significant negative correlations with SiO_2, TiO_2, Na_2O, Zr. and positive correlations with CaO, Mg#, Ni, Cr these correlations can be explained by the fractionation of plagioclase, clinopyroxene, amphibole, and Fe–Ti oxides.

There are good correlations between major and trace elements. The data on major and trace element chemistry of Qaladeza metabasalt suggest that mostly their protolith was quartz–normative calic alkaline basalt. Trace-element characteristics of the Qaladeza metabasalt further suggest that they resemble calic alkaline basalt REE patterns and tectonic settings diagrams confirm the trace element results, with a typical pattern for the subduction-zone system in Iraqi Zagros Zone, as indicated by whole rock trace element patterns typical for subduction-related magmas (negative Nb anomalies in Normal Mid Oceanic Ridge Basalt normalised diagrams, positive LREE/HFSE ratios).

ACKNOWLEDGEMENTS

Sample preparation and geochemical analyses was funded by Geoquest ,Wollongong University, Australia. Author would like to thank Professor Sabah Ismail, Kirkuk University and Professor Kamal Haji Karim, Sulaimani University, for their help in the field trip.

REFERENCES

[1] S. Z. Jassim and Goff C. (eds), ***Geology of Iraq.Dolin Prague and Moravian Museum***, Brno, 2006.

[2] S. Z. Jassim,Waldhausrova, J. and Suk, M, ***Evolusion of Magmatic Activity in Iraqi Zagros Complexes***. Krystalinikum, Vol. 16, pp. 87 – 108, 1982.

[3] T. Buday, ***Stratigraphy and Palaeogeography, The Regional Geology of Iraq 1.*** GEOSURV, Baghdad, 1980.

Kirkuk University Journal /Scientific Studies (KUJSS)
Volume 10, Issue 3, September 2015 , p.p(242-258)
ISSN 1992 – 0849

[4] S. A. Ali, S. Buckman, K. J. Aswad, B. G. Jones, S. A. Ismail, and A. P. Nutman, ***Recognition of Late Cretaceous Hasanbag Ophiolite-Arc Rocks in the Kurdistan Region of the Iraqi Zagros Thrust Zone***: A missing Link in the Paleogeography of the Closing Neo-Tethys Ocean. The Geological Society of America, Lithosphere doi:10.1130/L207.1, 2012.

[5] K. J. Aswad, N. R. H. Aziz,, and H. A. Koyi, ***Cr-spinel Compositions in Serpentinites and their Implications for the Petrotectonic History of the Zagros Suture Zone***, Kurdistan Region, Iraq. Geological Magazine 148, pp.802–18, 2011.

[6] N.R.H. Aziz, K.J. Aswad, and, H.Koyi, ***Contrasting of serpentinite bodies in northwestern Zagros Suture Zone serpentinites***, Kurdistan region, Iraq: tracing a "***subduction signature***" in serpentinite-matrix mélanges. Geological Magazine, 148, pp.819-837, 2011.

[7] K.J. Aswad, R.M. Al.Sheraefy, and S.A. Ali, ***Pre-collisional intrusive magmatism in the Bulfat Complex***, ***Wadi Rashid, Qala Deza, NE Iraq***: ***geochemical and mineralogical constraints and implications for tectonic evolution of granitoid-gabbro suites***. Iraqi National Journal of Earth Sciences, 13, pp.103-137, 2013.

[8] K.J. Aswad, ***Arc-continental collision in northeastern Iraq as evidence by the Mawat and Penjween ophiolite complex***. Rafidain Journal of Science, 10, pp.51-61, 1999.

[9] K. Norrish, and B.W. Chappell, ***X-ray fluorescence spectrometry***, in Zussman, J., ed., ***Physical Methods of Determinative Mineralogy (2nd ed.)***: London, Academic Press, pp. 201–272, 1977.

[10] S. A. Ali, ***Geochemistry and geochronology of Tethyan-Arc related igneous rocks***, NE-Iraq. NE Iraq. (PhD thesis), University of Wollongong, 326 p (unpublished), 2012.

[11] M. D. Foster, ***Interpretation of the Compositions of Lithium Micas.*** United States Professional Paper Geological Survey, Vol. 354-E, pp. 115 – 147, 1960.

[12] T.N. Irvine, and W.R.A. Baragar, ***A guide to the chemical classifi cation of the common volcanic rocks***: Canadian Journal of Earth Sciences, v. 8, p. 523–548, doi:10.1139 /e71-055, 1971.

[13] E.D. Mullen, ***MnO/TiO2/P2O5, a minor element discriminate for basaltic rocks of oceanic environments and its implications for petrogenesis***: Earth and Planetary Science Letters, v. 62, p. 53–62, doi:10.1016/0012-821X(83)90070-5, 1983.

[14] M. Wilson, ***Igneous Petrogenesis***. Unwin Hyman, London, 1989.

[15] M. Meschede, ***A method of discriminating between different types of mid-ocean ridge basalts and continental tholeiites with the Nb-1bZr-1bY diagram***: Chemical Geology, v. 56, p. 207–218, doi:10.1016/0009-2541(86)90004-5, 1986.

[16] N. Nakamura, ***Determination of REE, Ba, Fe, Mg, Na and K in carbonaceous andordinary chondritic meteorites***: Geochimica et Cosmochimica Acta, v. 38, pp. 757–775, doi:10.1016/0016-7037(74)90149-5, 1974.

[17] A. Wood, ***The application of a Th-Hf-Ta diagram to problems of tectonomagmatic classification and toestablishing the nature of crustal contamination of basaltic lavas of the British Tertiary Volcanic Province***.Earth and Planetary Science Letters 50, pp.11–30, 1980.

[18] J.A. Pearce, ***Role of the sub-continental lithosphere in magma genesis at active continental margins,*** in Continental Basalts and Mantle Xenoliths: Cheshire, UK, Shiva,pp. 230–249, 1983.

[19] M. J. Le Bas, R. W. Le Maitre, A. Streckeisen & B. Zanettin, ***A chemical classification of volcanic rocks based on the total alkali-silica diagram***. J Petrology 27: pp.745-750 doi: 10.1093/petrology/27.3.745, 1986.

[20] S. Sun and W. McDonough, ***Chemical and isotopic systematics of oceanic basalts***: ***Implications for mantle composition and processes***, in Saunders, A.D., and Norry, M.J., eds., Magmatism in the Ocean Basins: ***Geological Society of London Special Publication 42***, p. 313–345, 1989.

AUTHOR

Sarmad A. Ali: received B.Sc. and M.S. degrees in Geology from, Salahadeen University/Arbil-Iraq and Mosul University/Mosul-Iraq in 1990 and 2002, respectively. In 2012 received Ph.D. in Geochemistry from Wollongong University-Australia. At 2012 till now as an Assistant Professor in Applied Geology Department, College of Sciences, Kirkuk University.